

Tracking the dynamics of an ideal quantum measurement: Supplemental Material

Fabian Pokorny,^{1,*} Chi Zhang,^{1,†} Gerard Higgins,^{1,‡} Adán Cabello,^{2,3,§} Matthias Kleinmann,^{4,5,¶} and Markus Hennrich^{1,**}

¹*Department of Physics, Stockholm University, 10691 Stockholm, Sweden*

²*Departamento de Física Aplicada II, Universidad de Sevilla, E-41012 Sevilla, Spain*

³*Instituto Carlos I de Física Teórica y Computacional, Universidad de Sevilla, E-41012 Sevilla, Spain*

⁴*Department of Theoretical Physics, University of the Basque Country UPV/EHU, E-48080 Bilbao, Spain*

⁵*Naturwissenschaftlich-Technische Fakultät, Universität Siegen, 57068 Siegen, Germany*

MODEL FOR MEASUREMENT PROCESS

We consider the transition between a ground state $|0\rangle$ and a short-lived excited state $|e\rangle$ of the trapped ion. This transition is driven with Rabi frequency Ω using a classical laser field, where the laser frequency is detuned from resonance by Δ . In the rotating-wave approximation, the interaction Hamiltonian is then given by [1]

$$H_I = \hbar\Delta|e\rangle\langle e| + \frac{\hbar\Omega}{2}(\sigma_+ + \sigma_-), \quad (1)$$

written in the frame rotating with the laser field. Here, $\sigma_+ = |e\rangle\langle 0| = \sigma_-^\dagger$. The other levels used in our system, $|1\rangle$ and $|2\rangle$, are unaffected by the driving laser, so that H_I does not have contributions involving those levels.

The excited state decays back to the ground state with decay rate Γ and on decay, a photon is emitted into the photonic environment. In the Born–Markov approximation, this environment can be traced out and the state ρ of the levels $|0\rangle$, $|1\rangle$, $|2\rangle$, and $|e\rangle$ follows a master equation in Lindblad form [1]. In the interaction picture, this equation reads

$$\dot{\rho} = -\frac{i}{\hbar}[H_I, \rho] + \frac{\Gamma}{2}(2\sigma_- \rho \sigma_+ - \sigma_+ \sigma_- \rho - \rho \sigma_+ \sigma_-). \quad (2)$$

Without the laser ($\Omega = 0$) we have $\dot{\rho}_{e,e} = -\Gamma\rho_{e,e}$ and hence after a very short time ($\sim \Gamma^{-1}$) the excited state relaxes, $\rho_{e,e} = 0$. Since we assume that there was no population of the excited level in the initial state, it is sufficient to consider the qutrit part of ρ . The transformation Λ_m induced by the measurement is then

$$\Lambda_m[\rho] = \begin{pmatrix} \rho_{0,0} & \rho_{0,1} g_0 & \rho_{0,2} g_0 \\ \rho_{1,0} g_0^* & \rho_{1,1} & \rho_{1,2} \\ \rho_{2,0} g_0^* & \rho_{2,1} & \rho_{2,2} \end{pmatrix}, \quad (3)$$

in accordance with

$$\Lambda_m: \rho \mapsto \sqrt{E_1}\rho\sqrt{E_1} + G\sqrt{E_0}\rho\sqrt{E_0}G^\dagger. \quad (4)$$

The variable $g_0 \equiv g_0(t)$ is determined by the solution of the master equation Eq. (2) for $\rho_{0,1}$, namely,

$$\dot{\rho}_{0,1} = -i\frac{\Omega}{2}\rho_{e,1}, \quad (5)$$

$$\dot{\rho}_{e,1} = -i\frac{\Omega}{2}\rho_{0,1} - \left(\frac{\Gamma}{2} + i\Delta\right)\rho_{e,1}. \quad (6)$$

These equations can be solved exactly, but yield impractical expressions. However, for $\Omega \ll \Gamma$ the excited state can be adiabatically eliminated via $\dot{\rho}_{e,1} \approx 0$. With this approximation

$$g_0 \approx \exp\left(-\frac{\Omega^2}{2\Gamma + 4i\Delta}t\right) \cdot \exp(i\phi_r), \quad (7)$$

follows at once. The phase ϕ_r results from the ac-Stark shifts between $|0\rangle$ and $\{|1\rangle, |2\rangle\}$ induced by the 422 nm and 1092 nm laser fields. This effect prevents us from observing the natural phase of g_0 and for our study of the Lüders theory of measurement, it is not relevant. In the case of a full projection (meaning a measurement with an interaction strength of 100%), the amplitude of the coherence goes to zero and thus ϕ_r becomes irrelevant, see Eq. (3). For the other three measurements with interaction strength less than 100% this is not the case and we tune the intensities and detuning of the repump fields such that $\phi_r = 0$.

INITIAL STATE PREPARATION

j	U_j	$ \psi_j\rangle = U_j 0\rangle$
1	$\mathbb{1}$	$ 0\rangle$
2	$R_y^1(\pi)$	$ 1\rangle$
3	$R_y^2(\pi)$	$ 2\rangle$
4	$R_y^1(\pi/2)$	$\frac{1}{\sqrt{2}}(0\rangle + 1\rangle)$
5	$R_{-x}^1(\pi/2)$	$\frac{1}{\sqrt{2}}(0\rangle + i 1\rangle)$
6	$R_y^2(\pi/2)$	$\frac{1}{\sqrt{2}}(0\rangle + 2\rangle)$
7	$R_{-x}^2(\pi/2)$	$\frac{1}{\sqrt{2}}(0\rangle + i 2\rangle)$
8	$R_y^2(\pi)R_y^1(\pi/2)$	$\frac{1}{\sqrt{2}}(1\rangle + 2\rangle)$
9	$R_y^2(\pi)R_{-x}^1(\pi/2)$	$\frac{1}{\sqrt{2}}(1\rangle + i 2\rangle)$

TABLE I. Pulse sequences for the implementation of the unitaries U_j , as used for the preparation and measurement of the qutrit. $R_{\hat{n}}^\ell(\phi)$ is a rotation in the qutrit subspace spanned by $|0\rangle$ and $|\ell\rangle$ of angle ϕ about axis \hat{n} . The pulse sequence is applied from right to left.

	Power [μ W]	Ω [2π MHz]	P_{scatt}	F
(a)	0.08	1.3 ± 0.1	$(33^{+7}_{-6})\%$	0.94
(b)	0.16	1.9 ± 0.2	$(56^{+8}_{-9})\%$	0.95
(c)	0.48	3.2 ± 0.3	$(91^{+4}_{-6})\%$	0.93
(d)	10.75	15.2 ± 1.5	100%	0.94

TABLE II. Experimental settings: power of the laser used to drive the $|0\rangle \leftrightarrow |e\rangle$ transition measured directly before the experiment chamber, corresponding Rabi frequency Ω , photon scattering probability $P_{\text{scatt}} = 1 - |g_0|^2$, and experimental process fidelity F with the model process Λ_m . The infidelity is mainly caused by the finite linewidth of the 674 nm laser and magnetic field fluctuations. The statistical uncertainty of F is ± 0.01 .

EXPERIMENTAL SETTINGS

In order to track the dynamics of the Lüders process, we take four snapshots with varying measurement interaction strengths, i.e. varying 422 nm laser power. Table II shows the relevant parameters for each experiment with the resulting scattering probability P_{scatt} and fidelity F between the experimental process and the model process Λ_m . F is given by

$$F = \frac{1}{9} \left[\text{tr} \left(\sqrt{\sqrt{\chi_m} \chi_{\text{exp}} \sqrt{\chi_m}} \right) \right]^2, \quad (8)$$

with model Choi matrix χ_m and experimental Choi matrix χ_{exp} .

COMPARISON OF THE CHOI MATRIX RECONSTRUCTED FROM EXPERIMENT AND MODEL DATA

Fig. 1 shows the comparison of the Choi matrices χ_{exp} reconstructed from experimental data (see Fig. 2 in the main text) and Choi matrices χ_m predicted by our measurement model. For all four snapshots, the real part of the model (blue bars) and experiment (orange bars) as well as the imaginary part (green and red bars for model and experiment, respectively) are plotted. The average fidelity between model and experiment is 94%.

POST-PROCESS DENSITY MATRICES FOR A STATE WITH CONSERVED COHERENCE AND A STATE WITH DESTROYED COHERENCE

Fig. 2 shows the evolution of the initial qutrit states $\frac{1}{\sqrt{2}}(|1\rangle + i|2\rangle)$ [(a) – (d)] and $\frac{1}{\sqrt{2}}(|0\rangle + i|2\rangle)$ [(e) – (h)] with increasing coupling to the environment. State $\frac{1}{\sqrt{2}}(|1\rangle + i|2\rangle)$ is unaffected by the 422 nm laser field as it only affects $|0\rangle$. Thus the coherence between the states $|1\rangle$ and $|2\rangle$ is preserved. For the state $\frac{1}{\sqrt{2}}(|0\rangle + i|2\rangle)$, the coupling of $|0\rangle$ to the photon environment causes loss of coherence between $|0\rangle$ and $|2\rangle$.

* fabian.pokorny@fysik.su.se

† chi.zhang@fysik.su.se

‡ gerard.higgins@fysik.su.se

§ adan@us.es

¶ matthias.kleinmann@uni-siegen.de

** markus.hennrich@fysik.su.se

[1] H. Carmichael, *An Open Systems Approach to Quantum Optics* (Springer-Verlag, Berlin, 1993)

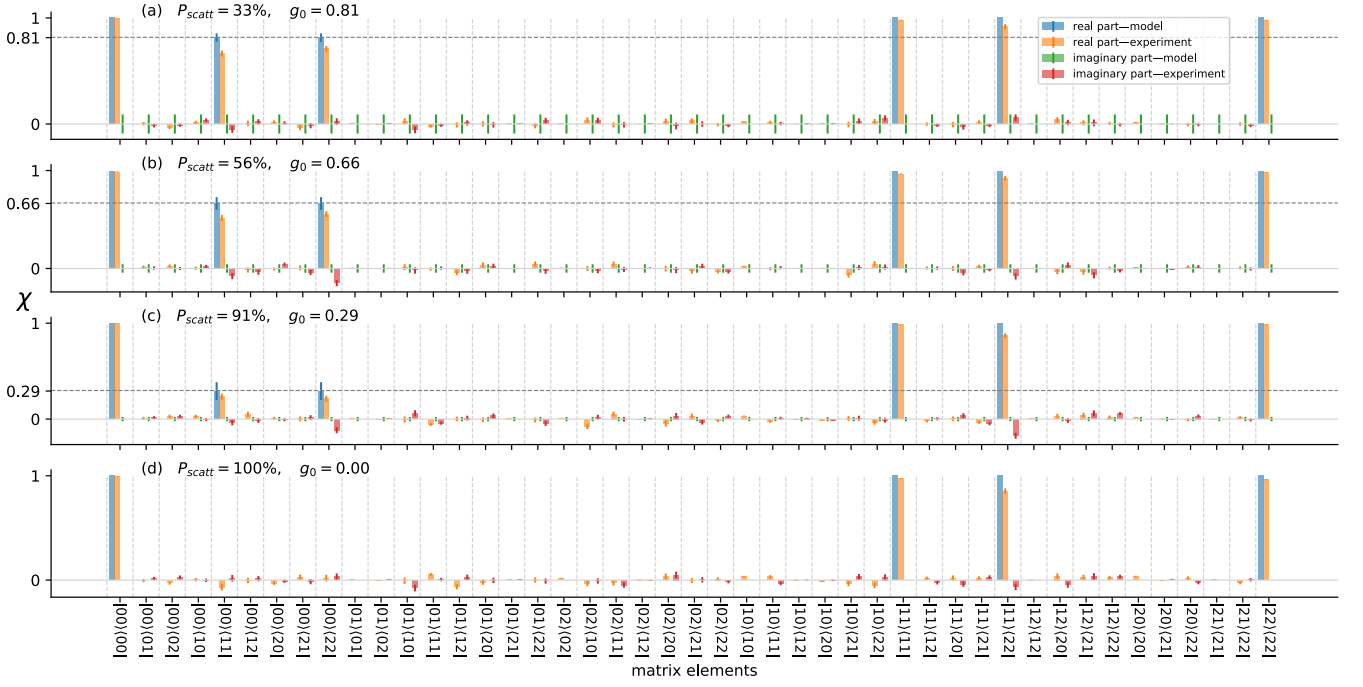


FIG. 1. Comparison of the elements of the experimentally-determined Choi matrices χ_{exp} and model predictions χ_m . From (a) to (d) the coupling strength of $|0\rangle$ to the photon environment is increased (see Table II) and coherences involving state $|0\rangle$ are destroyed. (d) is most similar to the ideal Lüders process, from (d) \rightarrow (a) the process becomes more similar to the trivial process $\rho \mapsto \rho$. Error bars in the model result from uncertainties in the experimental parameters Ω and Δ (68% confidence interval). Error bars in the experimentally-determined Choi matrix elements result from quantum projection noise (68% confidence interval).

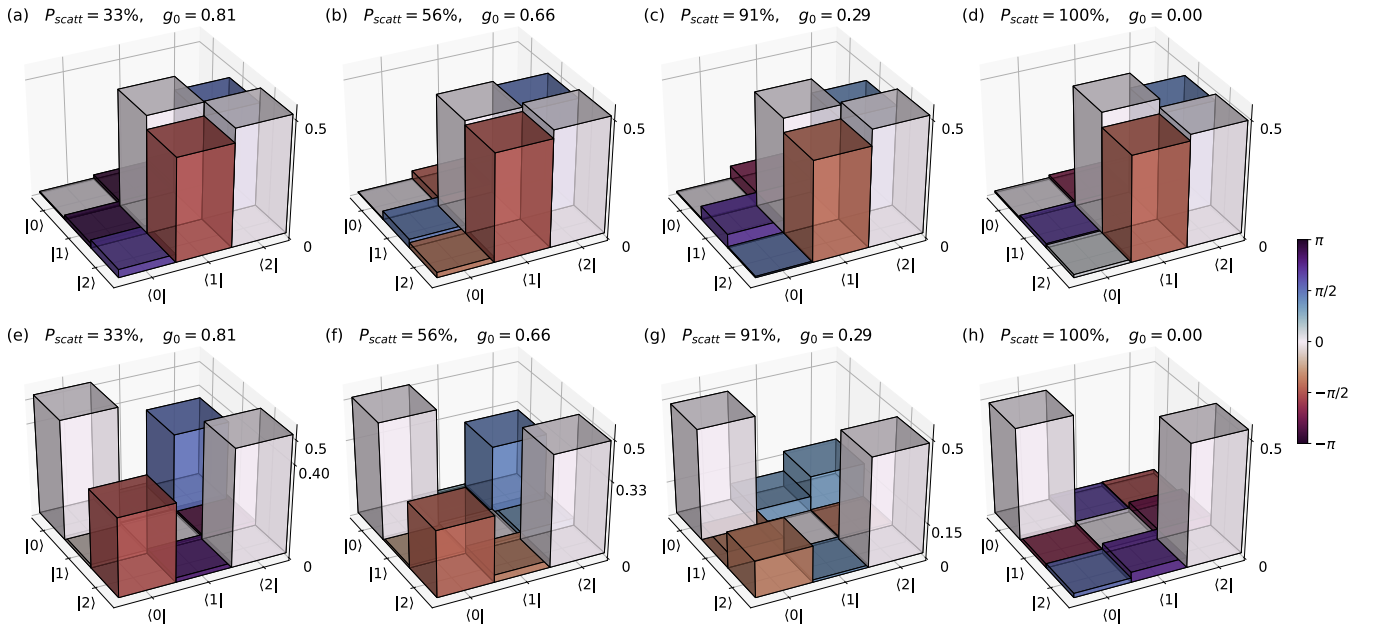


FIG. 2. Reconstructed density matrices ρ from the experimental data for the initial states $\frac{1}{\sqrt{2}}(|1\rangle + i|2\rangle)$ [(a) – (d)] and $\frac{1}{\sqrt{2}}(|0\rangle + i|2\rangle)$ [(e) – (h)]. The colors indicate the phase, g_0 is calculated according to our model, see Eq. (7). From (a) to (d) and from (e) to (h) the coupling strength of $|0\rangle$ to the photon environment is increased and coherences involving state $|0\rangle$ are destroyed. Thus the off-diagonal elements are preserved from (a) to (d) (state $\frac{1}{\sqrt{2}}(|1\rangle + i|2\rangle)$) while the off-diagonal elements decrease from (e) to (h) (state $\frac{1}{\sqrt{2}}(|0\rangle + i|2\rangle)$).